Reverse and Forward Engineering of Frequency Control in Power Networks

Lijun Chen and Seungil You

***Abstract*—We lay out a general framework for reverse-engineering frequency dynamics with general primary frequency control and frequency response, by showing that it is a distributed algorithm to solve a well-defined optimization problem. We further characterize the role of deadband in control, and show that if the aggregated uncontrolled load deviation is nonzero the frequencies will be synchronized, and if however it is zero the frequencies may oscillate but within the deadband. The optimization based model does not only provide a way to characterize the equilibrium and establish the convergence of the frequency dynamics, but also suggests a principled way to engineer frequency control. By leveraging the optimization problem and insights from reverse engineering, we design a distributed realtime frequency control scheme that maintains the frequency to the nominal value (i.e., frequency recovery) while achieves economic efficiency. This work presents a further step towards developing a new foundation – network dynamics as optimization algorithms – for distributed realtime control and optimization of future power networks.**

***Keywords*—Reverse and forward engineering, distributed control and optimization, network dynamics as optimization algorithms, frequency control, power networks.**

I. Introduction

The goal of frequency control is to balance power supply and demand to synchronize the frequency and maintain it to the nominal value. Traditionally, frequency control has a hierarchical structure that spans multiple timescales: primary control at subseconds to seconds, secondary control at seconds to minutes, and economic dispatch at minutes to hours; see, e.g., [24], [21]. The control at slow timescales (economic dispatch) is centralized and calculates set-points for the fast timescale control to track. Here economic efficiency is key, and the control is based on optimization models such as the optimal power flow (OPF) problem. On the other hand, the control at fast timescales (primary and secondary control) is local and automatic, usually oblivious of the global perspective such as economic efficiency. Here stability is key, and the design is based on dynamical models such as the swing equation. Such a control paradigm works well for today's system with relatively low uncertainty (large but slow and predictable variations, fast and unpredictable but small variations) and relatively small number of control points.

L. Chen is with Computer Science and Telecommunications, University of Colorado, Boulder, CO 80309, USA (email: lijun.chen@colorado.edu). S. You is with Control and Dynamical Systems, California Institute of Technology, Pasadena, CA 91125, USA (email: syou@caltech.edu).

The preliminary result of this paper has been presented at the IEEE Conference on Control and Decision (CDC), Los Angeles, California, December 2014.

However, the current control paradigm may be inadequate for the future power system. The future system expects to have rapid and large fluctuations in power supply/demand because of high penetration of renewable generation from solar and wind and active participation of end users. This implies that economic efficiency can not be ignored any more at fast timescales, and the fast timescale control needs to be bridged with systemwide properties such as economic efficiency. Moreover, the future system may consist of a huge number of control points, which implies that the control must be distributed and based on local information. It is however challenging to achieve systemwide properties through local controls/decisions for a large interconnected system such as the power network.

We aim to find a principled way to guide systematic design of local controls with global perspective for frequency control. The approach we take is reverse and forward engineering. We first develop models to understand the systemwide properties arising from the interaction among local controls, in particular, whether the power system dynamics with the existing controls can be interpreted as distributed algorithm for solving certain optimization problem, i.e., *network dynamics as optimization algorithms*. We then leverage the insights obtained from reverse engineering and engineer the optimization-based model to incorporate the desired objectives and proper constraints, and design distributed control scheme according to distributed algorithm for solving the resulting optimization problem.

Specifically, we first lay out a general framework for reverse-engineering frequency dynamics with general primary frequency control and frequency response, by showing that it is a partial primal-dual gradient algorithm for solving a well-defined optimization problem. We further characterize the role of deadband in control, and show that if the aggregated uncontrolled load deviation is nonzero the frequencies will be synchronized, and if however it is zero the frequencies may oscillate but within the deadband. The optimization-based model does not only provide a way to characterize the equilibrium and establish the convergence of frequency dynamics, but also suggests a principled way to engineer frequency control. Based on insights obtained from reverse engineering, we then impose additionally a set of constraints to the optimization problem to design a distributed realtime frequency control scheme that does not only maintain the frequency to the nominal value, but also achieves economic efficiency. This is drastically different from the current hierarchical control approach that addresses frequency regulation and economic efficiency at different timescales and with centralized control, and is what is needed for the future power system to cope with rapid and large fluctuations in supply and demand and manage a huge number of control points.

II. Related work

The similar idea of reverse and forward engineering was first proposed to understand dynamic behaviors of existing network protocols and guide systematic design of better or new ones in communication networks; see, e.g., [15], [20], [19], [10], [9]. This line of work has led to the development of a promising mathematical theory for communication network architecture and protocol design – layering as optimization decomposition; see, e.g., [13], [10], [8], [6]. The layering as optimization decomposition framework views various protocol layers as carrying out distributed computation over the network to optimize a global objective function. Different layers iterate on different subsets of decision variables to achieve individual optimality. Taken together, these local algorithms achieve a global objective. We aim to develop a similar framework – network dynamics as optimization algorithm – for distributed realtime control and optimization of power networks. There are, however, fundamental differences between power and communication networks, in particular, the control/operation of power network cannot be decoupled from the physics of electricity while the control/operation of communication network can be decoupled from the physics of information. This requires designing distributed optimization algorithms that exploit or can be implemented as power system dynamics.

There is extensive literature on frequency control. We only review those few that are most relevant [27], [25], [26], [17], [22], [12], [18]. This paper was originally motivated by [27], [26] that designs load side primary frequency control based on a partial primal-dual gradient algorithm for a cost minimization problem. References [27], [26] focus on only *frequency synchronization*, and contain implicitly a component of reverse engineering of the linear frequency response of frequency-sensitive loads but do not explain how to derive the corresponding cost functions. In contrast, our paper 1) lays out a general framework for reverse-engineering frequency dynamics with general primary frequency control and frequency response, 2) characterizes the role of deadband in control, and 3) leverages primary frequency control and the insights from the reverse engineering to design a distributed realtime control scheme that maintains the frequency to nominal value (i.e., *frequency recovery*) while achieves economic efficiency.

Another related work is our earlier work [17], [18] that reverse-engineers automatic generation control (secondary frequency control) and proposes a modified control scheme to achieve economic efficiency. Our current paper achieves the same goals but modifies the primary frequency control and thus works at a faster timescale. Other work that takes a similar approach or in a similar flavor includes [25] that uses a primal-dual decomposition approach to design a dynamic feedback controller for generation and loads in power networks with star topology, and [12] that proposes a distributed droop control architecture for frequency regulation and economic efficiency for microgrids. Our paper is different in network/application setting and model as well as algorithm design.

III. System Model

Consider a power network modeled by a connected graph $(\mathcal{N}, \mathcal{E})$, with a set $\mathcal{N}$ of buses or control areas and a set $\mathcal{E}$ of power lines connecting the buses. The power network is initially at a steady state (or equilibrium) at the nominal frequency ω^0 and with bus $i \in \mathcal{N}$ voltage magnitude v_i and nominal phase angle θ_i^0. All the variables introduced next will be deviations or revisions with respect to this steady state.

For each bus $i \in \mathcal{N}$, let ω_i denote the frequency deviation, P_i^I the uncontrolled load deviation, and P_i^S the frequency-sensitive load deviation. P_i^S can be modeled by

$$P_i^S = G_i(\omega_i), \tag{1}$$

where frequency response function G_i is Lipschitz continuous, strictly increasing, and with $G_i(0) = 0$. A linear approximation $G_i(\omega_i) = D_i\omega_i$, $D_i > 0$ is usually used in literature, but we do not make such an assumption. We may impose upper/lower bounds to P_i^S (as well as to P_i^M and P_i^R introduced later). But this will not change the results of this paper. So, we ignore these constraints for simplicity of presentation.

We denote by $\mathcal{N}^M$ and $\mathcal{N}^R$ the subsets of buses at which there is a synchronous mechanical generator and renewable generation respectively, and $\mathcal{N}^L$ the subset of buses that only have loads. For simplicity of presentation, we assume that $\mathcal{N}^M \cap \mathcal{N}^R = \emptyset$, but the results in this paper hold even when $\mathcal{N}^M$ and $\mathcal{N}^R$ overlap. We will first consider primary frequency control.[1] For each bus $i \in \mathcal{N}^M$, let P_i^M denote the mechanical power revision that is controlled by certain primary frequency control scheme with a deadband of $\delta_i \geq 0$

$$P_i^M = F_i(\omega_i), \tag{2}$$

where control function F_i is Lipschitz continuous, strictly decreasing in $(-\infty, -\delta_i/2) \cup (\delta_i/2, \infty)$ and zero in $[-\delta_i/2, \delta_i/2]$, and can be more general than the usual droop control

$$F_i(\omega_i) = \begin{cases} -S_i(\omega_i - \frac{\delta_i}{2}), & \omega_i \geq \frac{\delta_i}{2} \\ 0, & |\omega_i| < \frac{\delta_i}{2} \\ -S_i(\omega_i + \frac{\delta_i}{2}), & \omega_i \leq -\frac{\delta_i}{2} \end{cases}$$

with $S_i > 0$. For each bus $i \in \mathcal{N}^R$, let P_i^R denote the renewable power deviation that is controlled by certain primary frequency control scheme with a deadband of $\delta_i \geq 0$

$$P_i^R = H_i(\omega_i), \tag{3}$$

where control function H_i is Lipschitz continuous, strictly decreasing in $(-\infty, -\delta_i/2) \cup (\delta_i/2, \infty)$, and zero in $[-\delta_i/2, \delta_i/2]$. Such frequency regulation services by the renewable generation have been recommended or mandated in certain countries, see, e.g., [1], [2], and are an active research area, see, e.g., [23], [11], [7], [5].

For each link $(i, j) \in \mathcal{E}$, let P_{ij} denote the real power flow from bus i to bus j. Under the DC power flow approximation [3], the dynamics of branch flow can be written as

$$\dot{P}_{ij} \quad = \quad B_{ij}(\omega_i - \omega_j), \tag{4}$$

[1] In this paper we have focused on the generation-side frequency control. But the model and framework apply to the load-side frequency control too, as load can be seen as "negative" generation and vice versa. Also, we have used $P_i^S = G_i(\omega_i)$ to model the frequency-sensitive load, but it can model the frequency-based load control as well.

where $B_{ij} = \frac{v_i v_j}{x_{ij}} \cos(\theta_i^0 - \theta_j^0)$ with x_{ij} the reactance of power line (i,j). The frequency dynamics is given by

$$M_i \dot{\omega}_i = F_i(\omega_i) - G_i(\omega_i) - P_i^I - \sum_{\{j:(i,j)\in\mathcal{E}\}} P_{ij},\ i \in \mathcal{N}^M, \quad (5)$$

$$H_i(\omega_i) = G_i(\omega_i) + P_i^I + \sum_{\{j:(i,j)\in\mathcal{E}\}} P_{ij},\ i \in \mathcal{N}^R, \quad (6)$$

$$0 = G_i(\omega_i) + P_i^I + \sum_{\{j:(i,j)\in\mathcal{E}\}} P_{ij},\ i \in \mathcal{N}^L, \quad (7)$$

where equation (5) is the swing equation for a synchronous generator with inertia M_i and equations (6)-(7) are algebra equations from power balance.

We will next take a new perspective to understand the frequency dynamics (4)-(7) by showing that it can be seen as a distributed algorithm for solving a well-defined optimization problem (reverse engineering). We will then leverage the optimization model and insights from reverse engineering to design new frequency control scheme (forward engineering).

IV. Reverse Engineering

A. Frequency dynamics as primal-dual gradient algorithm

Equations (1)-(3) define a relation between the load or generation deviation and the frequency deviation. Define a disutility or cost function for the frequency-sensitive load

$$C_i^S(P_i^S) = \int_0^{P_i^S} G_i^{-1}(P_i) dP_i,\ i \in \mathcal{N}, \quad (8)$$

a cost function for mechanical power control

$$C_i^M(P_i^M) = -\int_0^{P_i^M} F_i^{-1}(P_i) dP_i,\ i \in \mathcal{N}^M, \quad (9)$$

and a cost function for renewable power control

$$C_i^R(P_i^R) = -\int_0^{P_i^R} H_i^{-1}(P_i) dP_i,\ i \in \mathcal{N}^R. \quad (10)$$

Notice that the inverses $F_i^{-1}(P_i)$ and $H_i^{-1}(P_i)$ take a set-value $[-\delta_i/2, \delta_i/2]$ at the "singular" point $P_i = 0$. However, for the integrals in (9) and (10) to be well-defined, a single value should be assigned at $P_i = 0$. As 0 is a limit of the integrals, any particular choice of value does not change the cost functions. For simplicity, we define $F_i^{-1}(0) = 0$ and $H_i^{-1}(0) = 0$. Functions $C_i^S(\cdot)$, $C_i^M(\cdot)$, and $C_i^R(\cdot)$ are all continuous and strictly convex, but $C_i^M(\cdot)$ and $C_i^R(\cdot)$ may not be differentiable at the origin in the presence of the deadband.[2] These functions depend only on the control functions and are independent of how the feedback signal ω_i is updated. They characterize certain "inherent" characteristics of load response or generation control, such as the economic cost incurred or the willingness/activeness (virtual cost) in control. In particular, the nominal frequency is the desired operating frequency so the frequency-sensitive load at the nominal frequency can be seen as the desired load. Since P_i^s can be seen as the load change because of the frequency deviation from the nominal value, C_i^S can be seen as disutility incurred in this change from the desired load. Also, a more (less) aggressive control function F_i or H_i will lead to a smaller (larger) C_i^M or C_i^R value. Therefore, C_i^M and C_i^R can be seen as the provisioning costs of the mechanical and renewable generations, since we can view a more (less) aggressive control function as a result of a lower (higher) cost. Mathematically, a main motivation for defining the cost function, take $C_i^M(\cdot)$ as an example, is to establish the equivalence between the control algorithm (2) and the distributed decision:

$$P_i^M = \arg\min_{P_i}\ C_i^M(P_i) + P_i\omega_i \quad (11)$$

for given frequency deviation ω_i.

With the above cost functions, we define a cost minimization problem for frequency control subject to the power balance:

$$\min_{\mathbf{P}^S,\mathbf{P}^M,\mathbf{P}^R,\mathbf{P}} \quad \sum_{i\in\mathcal{N}} C_i^S(P_i^S) + \sum_{i\in\mathcal{N}^M} C_i^M(P_i^M) + \sum_{i\in\mathcal{N}^R} C_i^R(P_i^R) \quad (12)$$

$$\text{subject to} \quad P_i^S + P_i^I + \sum_{\{j:(i,j)\in\mathcal{E}\}} P_{ij} = P_i^M,\ i \in \mathcal{N}^M \quad (13)$$

$$P_i^S + P_i^I + \sum_{\{j:(i,j)\in\mathcal{E}\}} P_{ij} = P_i^R,\ i \in \mathcal{N}^R \quad (14)$$

$$P_i^S + P_i^I + \sum_{\{j:(i,j)\in\mathcal{E}\}} P_{ij} = 0,\ i \in \mathcal{N}^L, \quad (15)$$

where $\mathbf{P}^S = \{P_i^S; i \in \mathcal{N}\}$, $\mathbf{P}^M = \{P_i^M; i \in \mathcal{N}^M\}$, $\mathbf{P}^R = \{P_i^R; i \in \mathcal{N}^R\}$, and $\mathbf{P} = \{P_{ij}; (i,j) \in \mathcal{E}\}$. The above convex optimization problem is actually a DC optimal power flow problem. Obviously, Slater's condition holds [4], i.e., there exists a feasible point for problem (12)-(15).

Introduce Lagrangian multiplier λ_i for each constraint of (13)-(15), and consider the Lagrangian

$$\begin{aligned} & L(\mathbf{P}^S, \mathbf{P}^M, \mathbf{P}^R, \mathbf{P}; \boldsymbol{\lambda}) \\ = & \sum_{i\in\mathcal{N}} C_i^S(P_i^S) + \sum_{i\in\mathcal{N}^M} C_i^M(P_i^M) + \sum_{i\in\mathcal{N}^R} C_i^R(P_i^R) \\ & - \sum_{i\in\mathcal{N}^M} \lambda_i (P_i^S + P_i^I + \sum_{\{j:(i,j)\in\mathcal{E}\}} P_{ij} - P_i^M) \\ & - \sum_{i\in\mathcal{N}^R} \lambda_i (P_i^S + P_i^I + \sum_{\{j:(i,j)\in\mathcal{E}\}} P_{ij} - P_i^R) \\ & - \sum_{i\in\mathcal{N}^L} \lambda_i (P_i^S + P_i^I + \sum_{\{j:(i,j)\in\mathcal{E}\}} P_{ij}), \end{aligned} \quad (16)$$

where $\boldsymbol{\lambda} = \{\lambda_i; i \in \mathcal{N}\}$. As Slater's condition holds, there exists a saddle point of L, i.e., a primal-dual optimum of problem (12)-(15) and its dual.

Define a reduced Lagrangian:

$$\hat{L}(\mathbf{P}; \boldsymbol{\lambda}^M) = \max_{\boldsymbol{\lambda}^R, \boldsymbol{\lambda}^L} \ \min_{\mathbf{P}^S, \mathbf{P}^M, \mathbf{P}^R} L(\mathbf{P}^S, \mathbf{P}^M, \mathbf{P}^R, \mathbf{P}; \boldsymbol{\lambda}), \quad (17)$$

where $\boldsymbol{\lambda}^M = \{\lambda_i; i \in \mathcal{N}^M\}$, $\boldsymbol{\lambda}^R = \{\lambda_i; i \in \mathcal{N}^R\}$, and $\boldsymbol{\lambda}^L = \{\lambda_i; i \in \mathcal{N}^L\}$, i.e., the dual variables corresponding to the

[2] In reverse engineering, we define cost functions for given control functions. In forward engineering (Section V), we can derive control functions for given cost functions, by "inverting" equations (8)-(10).

constraints (13), (14), and (15) respectively. We will study the saddle point dynamics for $\hat{L}$, which gives a partial primal-dual gradient algorithm for problem (12)-(15) and its dual.

Theorem 1. *The frequency dynamics* (4)-(7) *is a partial primal-dual gradient algorithm to solve problem* (12)-(15) *and its dual. Moreover, the set of saddle points of the Lagrangian L is the set of equilibira of dynamical system* (4)-(7).

Proof: For the inner minimization in (17), we have the first order optimality condition: $\partial_{P_i^S} C_i^S = \lambda_i,\ i \in \mathcal{N}$, $\partial_{P_i^M} C_i^M = -\lambda_i,\ i \in \mathcal{N}^M$ and $\partial_{P_i^R} C_i^R = -\lambda_i,\ i \in \mathcal{N}^R$, which, by the definition (8)-(10) of the cost functions, gives $P_i^S = G_i(\lambda_i),\ i \in \mathcal{N}$, $P_i^M = F_i(\lambda_i),\ i \in \mathcal{N}^M$ and $P_i^R = H_i(\lambda_i),\ i \in \mathcal{N}^R$. Let $\tilde{L}(\mathbf{P};\boldsymbol{\lambda}) = \min_{\mathbf{P}^S,\mathbf{P}^M,\mathbf{P}^R} L(\mathbf{P}^S,\mathbf{P}^M,\mathbf{P}^R,\mathbf{P};\boldsymbol{\lambda})$, which is concave by definition and continuously differentiable with respect to $\boldsymbol{\lambda}$ due to strict convexity of the cost function; see Proposition 6.1.1 in [4]. Thus, for the outer maximization in (17), we have first oder optimality condition $\partial_{\lambda_i} \tilde{L}(\mathbf{P};\boldsymbol{\lambda}) = 0, i \in \mathcal{N}^R \cup \mathcal{N}^L$, which gives

$$G_i(\lambda_i) + P_i^I + \sum_{\{j:(i,j)\in\mathcal{E}\}} P_{ij} - H_i(\lambda_i) = 0, i \in \mathcal{N}^R, \tag{18}$$

$$G_i(\lambda_i) + P_i^I + \sum_{\{j:(i,j)\in\mathcal{E}\}} P_{ij} = 0, i \in \mathcal{N}^L. \tag{19}$$

Apply the saddle point dynamics to the reduced Lagrangian $\hat{L}(\mathbf{P};\boldsymbol{\lambda}^M)$, we have

$$\dot{P}_{ij} = -\epsilon_{ij}\frac{\partial \hat{L}}{\partial P_{ij}} = \epsilon_{ij}(\lambda_i - \lambda_j),\ (i,j) \in \mathcal{E}, \tag{20}$$

$$\dot{\lambda}_i = \kappa_i \frac{\partial \hat{L}}{\partial \lambda_i} = \kappa_i (F_i(\lambda_i) - G_i(\lambda_i) - P_i^I - \sum_{\{j:(i,j)\in\mathcal{E}\}} P_{ij}),\ i \in \mathcal{N}^M, \tag{21}$$

where $\epsilon_{ij} > 0$ and $\kappa_i > 0$. Again, $\hat{L}$ is differentiable with respect to $\lambda_i,\ i \in \mathcal{N}^M$ due to the strict convexity of the cost function. Equations (18)-(21) are the dynamical equations (4)-(7) if identifying $\lambda_i = \omega_i$ and setting $\epsilon_{ij} = B_{ij}$ and $\kappa_i = \frac{1}{M_i}$. The second half of the theorem follows from the KKT condition for the saddle point [4]. ∎

B. Saddle points and convergence of frequency dynamics

We first characterize the saddle point of the Lagrangian L, i.e, the equilibrium of the frequency dynamics (4)-(7).

Proposition 2. *Let $\mathcal{S}$ be the set of saddle points of the Lagrangian L. If $(\mathbf{P}^S,\mathbf{P}^M,\mathbf{P}^R,\mathbf{P};\boldsymbol{\lambda}) \in \mathcal{S}$, then*

$$\lambda_i = \omega,\ i \in \mathcal{N}, \tag{22}$$

$$F_i(\lambda_i) = G_i(\lambda_i) + P_i^I + \sum_{\{j:(i,j)\in\mathcal{E}\}} P_{ij},\ i \in \mathcal{N}^M, \tag{23}$$

$$H_i(\lambda_i) = G_i(\lambda_i) + P_i^I + \sum_{\{j:(i,j)\in\mathcal{E}\}} P_{ij}, i \in \mathcal{N}^R, \tag{24}$$

$$0 = G_i(\lambda_i) + P_i^I + \sum_{\{j:(i,j)\in\mathcal{E}\}} P_{ij}, i \in \mathcal{N}^N, \tag{25}$$

where ω is a certain constant.

Proof: The result follows from the KKT condition. In particular, $\lambda_i = \lambda_j,\ \forall (i,j) \in \mathcal{E}$, which leads to (22). ∎

If the frequency dynamics converges to a saddle point, then the frequencies are synchronized and the supply and demand are balanced. But, in general we cannot guarantee the convergence, rather the dynamics converges to a compact subset of an invariant set $\mathcal{I}$; see Appendix of the technical report [28]. The set $\mathcal{I}$ is not necessarily contained in the set $\mathcal{S}$ of saddle points, nor is a singleton set which gives stability immediately. If however the synchronized frequency ω is uniquely determined, then $\mathcal{I}$ is contained in $\mathcal{S}$ and the frequency dynamics converges.

Lemma 3. *Suppose that ω in equation* (22) *is uniquely determined. Then the frequency dynamics* (4)-(7) *converges to a saddle point of Lagrangian L.*

Proof: The result follows from Proposition 14 in Appendix of [28]. ∎

A typical way to verify the uniqueness of ω is to check the strict concavity of the reduced Lagrangian $\tilde{L}(\mathbf{P};\boldsymbol{\lambda})$ in terms of $\boldsymbol{\lambda}$, which may not hold or may be difficult to check. An easy way is to exploit the power balance.

Theorem 4. *The frequency dynamics* (4)-(7) *converges to a saddle point of Lagrangian L.*

Proof: From the saddle point equations (22)-(25), we have the aggregate power balance: $\sum_{i\in\mathcal{N}} P_i^I = -\sum_{i\in\mathcal{N}} G_i(\omega) + \sum_{i\in\mathcal{N}^M} F_i(\omega) + \sum_{i\in\mathcal{N}^R} H_i(\omega)$. By the assumptions on functions G_i, F_i, H_i, the right hand side of the above equation is strictly decreasing. So, it has a unique solution. The result follows from Theorem 3. ∎

Notice that the *decoupling* structure of the optimization problem – the objective function being separable in the decision variables and the constraints involving only local variables or variables at neighboring network components – is key to deriving distributed algorithms. The problem (12)-(15) has the desired decoupling structure, as it has an *additive* objective function and *per-node* constraints. The Lagrangian multiplier λ_i is used to decouple those variables such as P_i^S, P_{ij} and P_i^M at a node i, and the update of λ_i involves only the variables local at that node. In the next section when we design new distributed algorithm, we make sure to preserve the decoupling structure of the problem, see the per-node constraints (27)-(29).

C. The impact of deadband

From the above discussion, it seems that the deadband in control does not bring any complication to frequency synchronization. This is because of the existence of frequency sensitive load, which ensures the uniqueness of ω, i.e., the synchronized frequency if the system converges. In order to study the impact of deadband, in this subsection we assume that there is no frequency sensitive load and there is a deadband in control, i.e., $\delta_i > 0$, for all $i \in \mathcal{N}^M \cup \mathcal{N}^R$.

Corollary 5. *If the aggregate uncontrolled load deviation is nonzero, i.e., $\sum_{i\in\mathcal{N}} P_i^I \neq 0$. Then the frequency dynamics*

(4)-(7) *converges to a saddle point of Lagrangian L in the presence of deadband in control.*

Proof: Let $\delta_m = \min_{i\in\mathcal{N}^M\cup\mathcal{N}^R} \delta_i$. Notice that $\sum_{i\in\mathcal{N}^M} F_i(\omega) + \sum_{i\in\mathcal{N}^R} H_i(\omega)$ is zero in $[-\delta_m/2, \delta_m/2]$ and strictly decreasing in $(-\infty, -\delta_m/2] \cup [\delta_m/2, \infty)$. If $\sum_{i\in\mathcal{N}} P_i^I \neq 0$, the aggregate power balance $\sum_{i\in\mathcal{N}} P_i^I = \sum_{i\in\mathcal{N}^M} F_i(\omega) + \sum_{i\in\mathcal{N}^R} H_i(\omega)$ has a unique solution for ω. The result follows from Theorem 3. ■

However, if the aggregate uncontrolled load deviation is zero, the convergence is not guaranteed because any $\omega \in [-\delta_m/2, \delta_m/2]$ satisfies the power balance. The system may oscillate, but this oscillation is confined within the deadband.

Theorem 6. *Suppose that the aggregate uncontrolled load deviation is zero, i.e., $\sum_{i\in\mathcal{N}} P_i^I = 0$. Then the frequencies are confined within the deadband at each bus.*

Proof: From the saddle point equations, there exists a saddle point $(\mathbf{P}^*, \boldsymbol{\lambda}^*)$ of $\hat{L}$ such that $\lambda_i^* = 0$, $P_i^I + \sum_{j:(i,j)\in\mathcal{E}} P_{ij}^* = 0$, $i \in \mathcal{N}$. Notice that $\hat{L}(\mathbf{P}^*, \boldsymbol{\lambda}^*) = 0$. As discussed in Appendix of [28], the saddle point dynamics eventually converges to an invariant set $\mathcal{I}$, and moreover, for any $(\mathbf{P}, \boldsymbol{\lambda}) \in \mathcal{I}$, we have $\hat{L}(\mathbf{P}^*, \boldsymbol{\lambda}^*) = \hat{L}(\mathbf{P}^*, \boldsymbol{\lambda})$ and $\hat{L}(\mathbf{P}, \boldsymbol{\lambda}^*) = \hat{L}(\mathbf{P}^*, \boldsymbol{\lambda}^*)$. From the former equality, we can conclude that $\lambda_i F_i(\lambda_i) = 0, i \in \mathcal{N}^M$ and $\lambda_i H_i(\lambda_i) = 0, i \in \mathcal{N}^R$. This implies $\lambda_i \in [-\delta_i/2, \delta_i/2]$ for all i. Therefore, at $\mathcal{I}$, all the frequencies are confined within the deadband. ■

D. Numerical example

We now use a numerical example to illustrate the analytical results established in the above. Consider a 4-area interconnected system as in Fig. 1, and assume that areas 1-3 have mechanical generators and area 4 has renewable generation. We use the linear approximation described after equation (1) for load frequency response function, and employ droop control of the same form as the example given after equation (2) for generators. The parameters used in simulations are shown in Tables I and II.

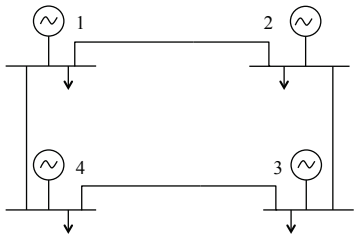

Fig. 1: A system with 4 control areas.

We consider three different scenarios. The first scenario corresponds to the case with frequency sensitive loads, and the second and third ones correspond to the cases without frequency sensitive loads and are used to illustrate the impact of the deadband. For the first two scenarios, we assume that the uncontrolled load deviates by 1pu at $t = 1s$ in the area 3, -0.5pu at $t = 5s$ in the area 2, and -1pu at $t = 10s$ in the area 1, thus the aggregate load deviation is nonzero after $t = 10s$. For the third scenario, we change the uncontrolled load deviation in area 1 from -1pu to -0.5pu so the aggregate load deviation is 0. Fig. 2 shows the frequency evolution. As expected, the frequencies are synchronized in the first two scenarios (Theorem 4 and Corollary 5), but oscillate within the deadband $[-0.1, 0.1]$ in the third one (Theorem 6).

Area j	M_j	D_j	$\lvert V_j\rvert$	S_j	δ_j
1	3	1	1.045	1	0.2
2	2.5	1.5	0.98	1	0.2
3	4	1.2	1.033	1	0.2
4	N/A	0.1	0.997	1	0.2

TABLE I: Generator Parameters

Line	1-2	2-3	3-4	4-1
B_{ij}	1	1	1	1

TABLE II: Line Parameters

Remark 7. *We have reverse-engineered frequency dynamics with general primary frequency control, by showing that it is a partial primal-dual gradient algorithm for solving a well-defined optimization problem. The optimization based model does not only provide a way to characterize the equilibrium and establish the convergence of frequency dynamics, but also suggests a principled way to engineer frequency control. New control scheme can be designed in a principled way by engineering the optimization problem and leveraging the insights from reverse engineering, as will be seen in the next section.*

V. Forward Engineering

In this section, we leverage the optimization based model and insights from reverse engineering to design a frequency control scheme that maintains the frequency to nominal value while achieves economic efficiency in a distributed real-time manner. The new control scheme is drastically different from the current hierarchical control approach that addresses frequency regulation and economic efficiency at different timescales and with centralized control.

Three key points from last section are: 1) network dynamics with frequency control is distributed algorithm solving an optimization problem; 2) the uniqueness of the dual optimum (i.e., the synchronized frequency) is the key to convergence; and 3) the synchronized frequency relates to the aggregate uncontrolled load deviation that frequency sensitive load and generation control need to balance. The first point suggests that we can design different control schemes to achieve different objectives, by decomposing the optimization problems that capture these objectives. The last two points suggest that the desired equilibrium $\omega = 0$ can be ensured if $\sum_{i\in\mathcal{N}} G_i(\omega) = 0$ at equilibrium. This leads to a constraint at equilibrium:

$$\sum_{i\in\mathcal{N}} P_i^I = \sum_{i\in\mathcal{N}^M} P_i^M + \sum_{i\in\mathcal{N}^R} P_i^R. \tag{26}$$

However, the above constraint couples the variables at all nodes of the network, and to impose it directly will change the

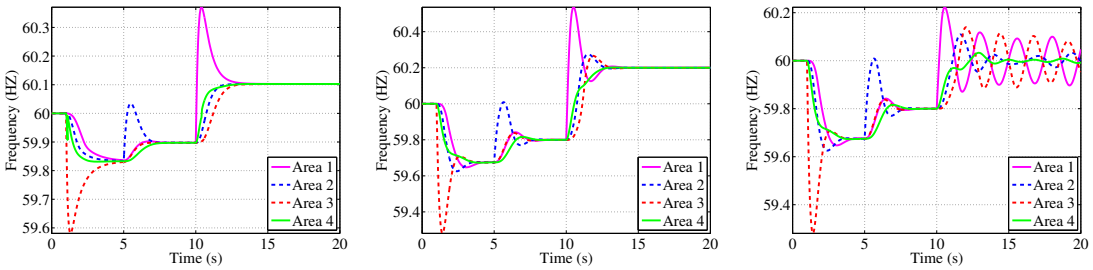

Fig. 2: The system with frequency sensitive loads (left panel), without frequency sensitive loads but with nonzero aggregate load deviation (middle panel) and with zero aggregate load deviation (right panel).

decoupling structure that enables distributed algorithm that is key to reverse engineering. We will instead impose it indirectly by imposing the following (decoupling) constrains:

$$P_i^M = P_i^I + \sum_{\{j:(i,j)\in\mathcal{E}\}} Q_{ij},\ i\in\mathcal{N}^M, \tag{27}$$

$$P_i^R = P_i^I + \sum_{\{j:(i,j)\in\mathcal{E}\}} Q_{ij},\ i\in\mathcal{N}^R, \tag{28}$$

$$0 = P_i^I + \sum_{\{j:(i,j)\in\mathcal{E}\}} Q_{ij},\ i\in\mathcal{N}^L, \tag{29}$$

where the slack variables Q_{ij} with $Q_{ij}=-Q_{ji}$ are introduced to ensure the constraint (26) through the *per-node* constraints. As the per-node constraints (13)-(15), the constraints (27)-(29) have the desired decoupling structure. This decoupling structure allows the design of distributed algorithm, as seen in Section IV and will be seen later.

Consider the following optimization problem, which is problem (12)-(15) with additionally constraints (27)-(29):

$$\min_{\mathbf{P}^S,\mathbf{P}^M,\mathbf{P}^R,\mathbf{P},\mathbf{Q}} \sum_{i\in\mathcal{N}} C_i^S(P_i^S)+\sum_{i\in\mathcal{N}^M} C_i^M(P_i^M)+\sum_{i\in\mathcal{N}^R} C_i^R(P_i^R) \tag{30}$$

$$\text{subject to}\quad (13)-(15)\ \&\ (27)-(29) \tag{31}$$

where $\mathbf{Q}=\{Q_{ij};(i,j)\in\mathcal{E}\}$. As in Section IV, introduce Lagrangian multipliers $\boldsymbol{\lambda}=\{\lambda_i;i\in\mathcal{N}\}$ for constraints (13)-(15) and $\boldsymbol{\mu}=\{\mu_i;i\in\mathcal{N}\}$ for (27)-(29), we define a Lagrangian $L(\mathbf{P}^S,\mathbf{P}^M,\mathbf{P}^R,\mathbf{P},\mathbf{Q};\boldsymbol{\lambda},\boldsymbol{\mu})$ and a reduced Lagrangian

$$\begin{aligned}&\hat{L}(\mathbf{P},\mathbf{Q};\boldsymbol{\lambda}^M,\boldsymbol{\mu})\\ =\ &\max_{\boldsymbol{\lambda}^R,\boldsymbol{\lambda}^L}\ \min_{\mathbf{P}^S,\mathbf{P}^M,\mathbf{P}^R} L(\mathbf{P}^S,\mathbf{P}^M,\mathbf{P}^R,\mathbf{P},\mathbf{Q};\boldsymbol{\lambda},\boldsymbol{\mu}).\end{aligned}$$

Consider the saddle point dynamics for $\hat{L}$:

$$\dot{\lambda}_i=\kappa_i(F_i(\lambda_i+\mu_i)-G_i(\lambda_i)-P_i^I-\sum_{\{j:(i,j)\in\mathcal{E}\}}P_{ij}),\ i\in\mathcal{N}^M, \tag{32}$$

$$0=G_i(\lambda_i)+P_i^I+\sum_{\{j:(i,j)\in\mathcal{E}\}}P_{ij}-H_i(\lambda_i+\mu_i),\ i\in\mathcal{N}^R \tag{33}$$

$$0=G_i(\lambda_i)+P_i^I+\sum_{\{j:(i,j)\in\mathcal{E}\}}P_{ij},\ i\in\mathcal{N}^L, \tag{34}$$

$$\dot{P}_{ij}=\epsilon_{ij}(\lambda_i-\lambda_j),\ (i,j)\in\mathcal{E}, \tag{35}$$

$$\dot{\mu}_i=\xi_i(F_i(\lambda_i+\mu_i)-P_i^I-\sum_{\{j:(i,j)\in\mathcal{E}\}}Q_{ij}),\ i\in\mathcal{N}^M, \tag{36}$$

$$\dot{\mu}_i=\xi_i(H_i(\lambda_i+\mu_i)-P_i^I-\sum_{\{j:(i,j)\in\mathcal{E}\}}Q_{ij}),\ i\in\mathcal{N}^R, \tag{37}$$

$$\dot{\mu}_i=-\xi_i(P_i^I+\sum_{\{j:(i,j)\in\mathcal{E}\}}Q_{ij}),\ i\in\mathcal{N}^L, \tag{38}$$

$$\dot{Q}_{ij}=\varepsilon_{ij}(\mu_i-\mu_j),\ (i,j)\in\mathcal{E}, \tag{39}$$

where $\kappa_i>0$, $\epsilon_{ij}>0$, $\xi_i>0$, and $\varepsilon_{ij}>0$. This saddle point dynamics gives the frequency dynamics under a new frequency control scheme, if identifying $\lambda_i=\omega_i$ and setting $\epsilon_{ij}=B_{ij}$ and $\kappa_i=\frac{1}{M_i}$. With this understanding, we will also refer it as the frequency dynamics and use λ_i and ω_i interchangeably.

Proposition 8. *Let $\mathcal{S}$ be the set of saddle points of the Lagrangian L. If $(\mathbf{P}^S,\mathbf{P}^M,\mathbf{P}^R,\mathbf{P},\mathbf{Q};\boldsymbol{\lambda},\boldsymbol{\mu})\in\mathcal{S}$, then*

$$\begin{aligned}&\omega_i=\omega,\ \mu_i=\gamma,\ i\in\mathcal{N},\\ &F_i(\gamma)=P_i^I+\sum_{\{j:(i,j)\in\mathcal{E}\}}P_{ij},\ i\in\mathcal{N}^M,\\ &H_i(\gamma)=P_i^I+\sum_{\{j:(i,j)\in\mathcal{E}\}}P_{ij},\ i\in\mathcal{N}^R,\\ &0=P_i^I+\sum_{\{j:(i,j)\in\mathcal{E}\}}P_{ij},\ i\in\mathcal{N}^N,\end{aligned} \tag{40}$$

where $\omega=0$ and γ is a certain constant.

Proof: The result follows from the KKT condition for the saddle point. In particular, $\omega_i=\omega_j$ and $\mu_i=\mu_j$ for all $(i,j)\in\mathcal{E}$, which leads to the first equation of (40). Also,

$$F_i(\omega+\gamma)=G_i(\omega)+P_i^I+\sum_{\{j:(i,j)\in\mathcal{E}\}}P_{ij},\ i\in\mathcal{N}^M, \tag{41}$$

$$H_i(\omega+\gamma)=G_i(\omega)+P_i^I+\sum_{\{j:(i,j)\in\mathcal{E}\}}P_{ij},\ i\in\mathcal{N}^R, \tag{42}$$

$$0 = G_i(\omega) + P_i^I + \sum_{\{j:(i,j)\in\mathcal{E}\}} P_{ij},\ i \in \mathcal{N}^N, \tag{43}$$

$$F_i(\omega+\gamma) = P_i^I + \sum_{\{j:(i,j)\in\mathcal{E}\}} Q_{ij},\ i \in \mathcal{N}^M, \tag{44}$$

$$H_i(\omega+\gamma) = P_i^I + \sum_{\{j:(i,j)\in\mathcal{E}\}} Q_{ij},\ i \in \mathcal{N}^R, \tag{45}$$

$$0 = P_i^I + \sum_{\{j:(i,j)\in\mathcal{E}\}} Q_{ij},\ i \in \mathcal{N}^N. \tag{46}$$

From the above equations, we get $\sum_{i\in\mathcal{N}} G_i(\omega) = 0$, which implies $\omega = 0$ since G_i is strictly monotone with $G_i(0) = 0$. Plugging $\omega = 0$ into (41)-(43), we conclude the proof. ■

The above proposition says that at a saddle point, i.e., an equilibrium of the frequency dynamics (32)-(39), the frequencies are synchronized to the nominal value. Notice that the strict monotonicity of G_i can only ensure the uniqueness in ω but not in γ, so it is inadequate to guarantee the convergence of frequency dynamics as in Section IV-B. Here the situation becomes similar to that in Section IV-C.

Theorem 9. *If the aggregate uncontrolled load deviation is nonzero, i.e., $\sum_{i\in\mathcal{N}} P_i^I \neq 0$, then the frequency dynamics* (32)-(39) *converges to a saddle point of Lagrangian L in the presence of deadband in control.*

Proof: Let $\delta_m = \min_{i\in\mathcal{N}^M\cup\mathcal{N}^R} \delta_i$. Notice that $\sum_{i\in\mathcal{N}^M} F_i(\gamma) + \sum_{i\in\mathcal{N}^R} H_i(\gamma)$ is zero in $[-\delta_m/2, \delta_m/2]$ and strictly decreasing in $(-\infty, -\delta_m/2] \cup [\delta_m/2, \infty)$. If $\sum_{i\in\mathcal{N}} P_i^I \neq 0$, the aggregate power balance $\sum_{i\in\mathcal{N}} P_i^I = \sum_{i\in\mathcal{N}^M} F_i(\gamma) + \sum_{i\in\mathcal{N}^R} H_i(\gamma)$ has a unique solution for γ. The convergence follows from Proposition 14 in Appendix of [28]. ■

Theorem 10. *Suppose that the aggregate uncontrolled load deviation is zero, i.e., $\sum_{i\in\mathcal{N}} P_i^I = 0$. Then the frequencies will be confined within the deadband at each bus.*

Proof: The proof is similar to that of Theorem 6. ■

Lastly, at an equilibrium, the system achieves economic efficiency, the goal of tertiary frequency control.

Theorem 11. *If it converges, the frequency dynamics* (32)-(39) *solves the following economic dispatch problem:*

$$\min_{\mathbf{P}^M,\mathbf{P}^R,\mathbf{P}} \quad \sum_{i\in\mathcal{N}^M} C_i^M(P_i^M) + \sum_{i\in\mathcal{N}^R} C_i^R(P_i^R) \tag{47}$$

subject to

$$P_i^I + \sum_{\{j:(i,j)\in\mathcal{E}\}} P_{ij} = P_i^M,\ i \in \mathcal{N}^M \tag{48}$$

$$P_i^I + \sum_{\{j:(i,j)\in\mathcal{E}\}} P_{ij} = P_i^R,\ i \in \mathcal{N}^R \tag{49}$$

$$P_i^I + \sum_{\{j:(i,j)\in\mathcal{E}\}} P_{ij} = 0,\ i \in \mathcal{N}^L. \tag{50}$$

Proof: Notice that the saddle point condition (40) is the KKT condition for problem (47)-(50) and its dual, with μ_i's the dual optimum. ■

From the above discussions, the partial primal-dual algorithm (32)-(39) suggests a realtime frequency control that synchronizes the frequency to nominal value and achieves economic efficiency at the same time. Moreover, as will be discussed next, the control is also distributed. Such a distributed realtime control is drastically different from the current hierarchical control approach that addresses frequency regulation and economic efficiency at different timescales, and is what is needed for the future power system to cope with rapid and large fluctuations in supply/demand and manage a huge number of control points.

A. Implementation

Notice that the frequency control scheme in (32)-(39) cannot be implemented directly, as P_i^I, which is usually unknown and time-varying, is needed for updating μ_i. However, if we choose $\xi_i = 1/M_i,\ i \in \mathcal{N}^M$ and let $\nu_i = \omega_i - \mu_i,\ i \in \mathcal{N}^M$, we can replace equation (36) by

$$\dot{\nu}_i = -\frac{1}{M_i}(G_i(\omega_i) + \sum_{\{j:(i,j)\in\mathcal{E}\}} (P_{ij} - Q_{ij})),\ i \in \mathcal{N}^M, \tag{51}$$

obtained by substracting (36) from (32). Moreover, we can solve for $P_i^I,\ i \in \mathcal{N}^R \cup \mathcal{N}^L$ from power balance equations (33)-(34), and implement equations (37)-(38) as

$$\dot{\mu}_i = \xi_i(G_i(\omega_i) + \sum_{\{j:(i,j)\in\mathcal{E}\}} (P_{ij} - Q_{ij})),\ i \in \mathcal{N}^R \cup \mathcal{N}^L. \tag{52}$$

To summarize, our proposed power control scheme for frequency control is as follows:

$$\begin{gathered} P_i^M = F_i(2\omega_i - \nu_i),\ i \in \mathcal{N}^M, \\ P_i^R = H_i(\omega_i + \mu_i),\ i \in \mathcal{N}^R, \\ (51) - (52), \\ \dot{Q}_{ij} = \varepsilon_{ij}(\mu_i - \mu_j),\ (i,j) \in \mathcal{E}, \end{gathered}$$

where in the last equation, $\mu_i = \omega_i - \nu_i$ if $i \in \mathcal{N}^M$. Notice that frequencies ω_i and branch flows P_{ij} can be measured locally, the frequency response G_i can be learned locally, and variables ν_i, μ_i, Q_{ij} can be calculated with local information at the buses. So, the above frequency control is distributed.

B. Numerical example

We test the above new frequency control scheme with the system shown in Fig. 1. We assume the same uncontrolled load deviations as those in the first two scenarios and the same generator parameters as in Table I in Section IV-D. We consider two different sets of line parameters: those in Table II and more realistic parameters in Table III. Fig. 3 shows the frequency evolution. We see that the new control scheme quickly recovers the nominal frequency. The reason to use two different sets of line parameters is to illustrate the impact of the B_{ij} magnitudes on the convergence speed. The fast synchronization shown in right panel is a result from large coupling coefficients B_{ij} between different areas.

Line	1-2	2-3	3-4	4-1
B_{ij}	26.5311	34.4333	17.2802	21.9803

TABLE III: Line Parameters

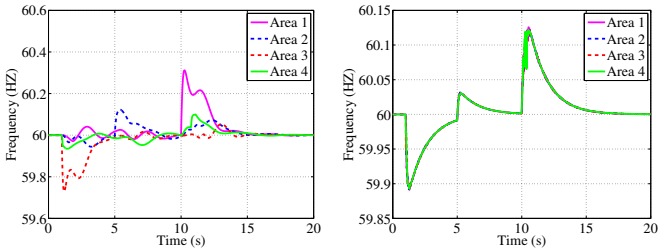

Fig. 3: Frequency dynamics with the new control scheme with line parameters in Table II (left) and in Table III (right).

VI. Conclusion

We have laid out a general framework for reverse-engineering frequency dynamics with general primary frequency control and frequency response, by showing that it is a distributed algorithm to solve a well-defined optimization problem. We have also characterized the role of deadband in control, and showed that if the aggregated uncontrolled load deviation is nonzero the frequencies will be synchronized, and if however it is zero the frequencies may oscillate but within the deadband. By leveraging the optimization problem and insights from reverse engineering, we have designed a distributed realtime frequency control scheme that does not only maintain the frequency to the nominal value, but also achieve economic efficiency. This is drastically different from the current hierarchical control approach that addresses frequency regulation and economic efficiency at different timescales and with centralized control, and is what is needed for future power system to cope with rapid and large fluctuations in supply/demand and manage a huge number of control points. Together with [27], [26], [17], [25], [12], [18], this work presents a step towards developing a new foundation – network dynamics as optimization algorithm – for distributed real-time control and optimization of future power networks.

Appendix: Saddle Point Dynamics

Consider a Lagrangian $L(x,y)$, corresponding to a (convex) constrained minimization problem $\mathcal{P}$ over x [4]. So, L is convex in primal variable x and concave in dual variable y. Assume that L is differentiable and ∇L is locally Lipschitz, and furthermore, L has a saddle point (x^*,y^*), i.e.,

$$L(x^*,y) \le L(x^*,y^*) \le L(x,y^*).$$

A saddle point gives a primal-dual optimum of problem $\mathcal{P}$ and its dual [4]. We denote by $\mathcal{S}$ the set of saddle points of L. We will study the saddle point dynamics $\mathcal{F}$:

$$\begin{aligned}\dot{x} &= -\Gamma_x \frac{\partial L}{\partial x},\\ \dot{y} &= \Gamma_y \frac{\partial L}{\partial y},\end{aligned}$$

where Γ_x and Γ_y are positive definite matrices. The saddle point dynamics corresponds to the primal-dual gradient algorithm for solving $\mathcal{P}$ and its dual. The case with $L \in \mathcal{C}^2$ has been studied in [14], but here we want to generalize to the case where L is differentiable and ∇L is locally Lipschitz but not necessarily differentiable. References [26], [18] also study a similar dynamics, corresponding to the case where L is strictly concave in y and the generation cost function is differentiable. Neither of these two properties is necessarily true in our case. These subtle differences have an outcome on convergence and require a refinement of the results in [14], [26], [18], although the details are in the same spirit.

Define a Lyapunov function

$$\begin{aligned}&U(x,y;x^*,y^*)\\ =\ &\frac{1}{2}((x-x^*)^T\Gamma_x^{-1}(x-x^*)+(y-y^*)^T\Gamma_y^{-1}(y-y^*))\end{aligned}$$

and consider its Lie-derivative $\mathcal{L}_{\mathcal{F}}U(x,y;x^*,y^*)$ along the flow generated by the differential equation $\mathcal{F}$:

$$\begin{aligned}&\mathcal{L}_{\mathcal{F}}U(x,y;x^*,y^*)\\ =\ &\left[-\Gamma_x\frac{\partial L}{\partial x}\quad \Gamma_y\frac{\partial L}{\partial y}\right]^T\left[\Gamma_x^{-1}(x-x^*)\quad \Gamma_y^{-1}(y-y^*)\right]\\ =\ &-\frac{\partial L}{\partial x}^T(x-x^*)+\frac{\partial L}{\partial y}^T(y-y^*)\\ \le\ &-L(x,y)+L(x^*,y)+L(x,y)-L(x,y^*)\\ =\ &L(x^*,y)-L(x,y^*)\\ =\ &L(x^*,y)-L(x^*,y^*)+L(x^*,y^*)-L(x,y^*)\\ \le\ &0,\end{aligned}$$

where the first inequality comes from the fact that L is convex in x and concave in y, and the last inequality from (x^*,y^*) being a saddle point of L. Notice that if $\mathcal{L}_{\mathcal{F}}U(x,y;x^*,y^*)=0$, then all the inequalities become equality, and $L(x^*,y)=L(x^*,y^*)$ and $L(x^*,y^*)=L(x,y^*)$. From LaSalle's invariance principle [16], the trajectory of $\mathcal{F}$ will be eventually contained in a compact subset of the invariant set

$$\mathcal{I}=\{(x,y):\mathcal{L}_{\mathcal{F}}U(x,y;x^*,y^*)=0\}.$$

The invariance set $\mathcal{I}$ may not be a subset of the set $\mathcal{S}$ of all saddle points of L, which means that the trajectory is bounded but may not converge. For example, suppose $L(x,y)=x^Ty$. Then $\mathcal{S}=\{(0,0)\}$ and the dynamics is given by: $\dot{x}=-y$, $\dot{y}=x$. The system oscillates around $(0,0)$ unless it is initially at $(0,0)$, and the trajectory is bounded but $\mathcal{I}$ is not contained in $\mathcal{S}$.

In order to ensure that the invariance set $\mathcal{I}$ is contained in the saddle point set $\mathcal{S}$, we can impose further constraint.

Proposition 12. *Suppose $L(x^*,\cdot)$ has a unique maximizer y^* or $L(\cdot,y^*)$ has a unique minimizer x^*. If $(x,y)\in\mathcal{I}$, then $(x,y)\in\mathcal{S}$.*

Proof: If $(x,y)\in\mathcal{I}$, then $L(x^*,y)=L(x^*,y^*)$ and $L(x^*,y^*)=L(x,y^*)$. By the assumption on L, either $x=x^*$ or $y=y^*$. Suppose $x=x^*$. Since $L(x,y)=L(x^*,y)=L(x^*,y^*)$, y is a maximizer of $L(x,\cdot)$. Moreover, since $x=x^*$ which is a constant, $\dot{x}=0$. This means that $-\Gamma_x\frac{\partial L}{\partial x}=0$, i.e., x

satisfies a first order optimality condition for $L(\cdot, y)$. Therefore x is also a minimizer of $L(\cdot, y)$, and hence (x, y) is a saddle point of L. Similarly, if $y = y^*$, we can also show that (x, y) is a saddle point of L. ■

The following result is immediate.

Proposition 13. *Suppose $L(x^*, \cdot)$ has a unique maximizer y^* or $L(\cdot, y^*)$ has a unique minimizer x^*. Then, the saddle point dynamics $\mathcal{F}$ asymptotically converges to a compact subset of $\mathcal{S}$.*

However, the above result does not give a pointwise convergence, which will be ensured in the following proposition.

Proposition 14. *Suppose $L(x^*, \cdot)$ has a unique maximizer y^* or $L(\cdot, y^*)$ has a unique minimizer x^*. Then, the saddle point dynamics $\mathcal{F}$ asymptotically converges to a saddle point $(x^*, y^*) \in \mathcal{I}$.*

Proof: Since $(x(t), y(t))$ converges to a compact subset of $\mathcal{I}$, there exists a subsequence $\{(x_k, y_k)\}$ where $x_k = x(t_k)$ and $y_k = y(t_k)$ that converges to a point (x^∞, y^∞). This implies that $u_k = U(x_k, y_k; x^\infty, y^\infty)$ converges to 0 asymptotically. Since $(x(t), y(t))$ will eventually be contained in $\mathcal{S}$, we have

$$\lim_{t\to\infty} U(x(t), y(t); x^\infty, y^\infty) = \lim_{t\to\infty} u(t) = u_\infty,$$

where u_∞ is a certain constant. However, as u_k is a subsequence of $u(t)$ and converges to 0, u_∞ should be 0. This concludes the proof. ■

REFERENCES

[1] Technical requirements for the connection of generation facilites to the hydro-quebec transmission system: Supplementary requirements for wind generation. *Technical Report*, Hydro-Quebec, Canada, 2005.

[2] Technical requirements for wind power and photovoltaic installations and any generating facilities whose technology does not consist of a synchronous generator directly connected to the grid. *Technical Report*, Red Electrica, Madrid, Spain, 2008.

[3] A. R. Bergen and V. Vittal. *Power Systems Analysis*. Pearson/Prentice Hall, 2000.

[4] D. Bertsekas. *Nonlinear programming*. Athena Scientific, 1999.

[5] A. Buckspan, J. Aho, P. Fleming, Y. Jeong, and L. Pao. Combining Droop Curve Concepts with Control Systems for Wind Turbine Active Power Control. *Proceedings of IEEE Symposium on Power Electronics and Machines in Wind Applications*, 2012.

[6] F. Chandra, D. F. Gayme, L. Chen, and J. C. Doyle. Robustness, Optimization, and Architecture. *European Journal of Control*, 5(6):472–482, 2011.

[7] L.-R. Chang-Chien, C.-M. Hung, and Y.-C. Yin. Dynamic reserve allocation for system contingency by dfig wind farms. *IEEE Transactions on Power Systems*, 23:729736, 2008.

[8] L. Chen, S. H. Low, and J. C. Doyle. Cross-Layer Design in Multihop Wireless Networks (Invited). *Special Issue on Wireless for the Future Internet, Computer Networks Journal*, 55(2):480–496, 2010.

[9] L. Chen, S. H. Low, and J. C. Doyle. Random Access Game and Medium Access Control Design. *ACM/IEEE Transactions on Networking*, 18(4):1303–1316, 2010.

[10] M. Chiang, S.H. Low, A.R. Calderbank, and J.C. Doyle. Layering as optimization decomposition. *IEEE Proceedings*, 95, 2007.

[11] R. de Almeida and J. P. Lopes. Participation of doubly fed induction wind generators in system frequency regulation. *IEEE Transactions on Power Systems*, 22:944950, 2007.

[12] F. Dorfler, J. W. Simpson-Porco, and F. Bullo. Breaking the hierarchy: Distributed control & economic optimality in microgrids. *IEEE Transactions on Control of Network Systems*, to appear, 2016.

[13] J. C. Doyle, J. Carlson, S. H. Low, F. Paganini, G. Vinnicombe, W. Willinger, J. Hickey, P. A. Parrilo, and L. Vandenberghe. Robustness and the Internet: Theoretical foundations. In E. Jen, editor, *Robust design: A repertoire from biology, ecology, and engineering*. Oxford University Press, 2003.

[14] D. Feijer and F. Paganini. Stability of primal–dual gradient dynamics and applications to network optimization. *Automatica*, 46(12):1974–1981, 2010.

[15] F. P. Kelly, A. K. Maulloo, and D. K. H. Tan. Rate control for communication networks: Shadow prices, proportional fairness and stability. *Journal of Operations Research Society*, 49:237–252, 1998.

[16] H. K. Khalil and J. W. Grizzle. *Nonlinear systems*, volume 3. Prentice hall Upper Saddle River, 2002.

[17] N. Li, L. Chen, C. Zhao, and S. H. Low. Connecting Automatic Generation Control and Economic Dispatch from an Optimization View. *Proceedings of American Control Conference*, 2014.

[18] N. Li, C. Zhao, and L. Chen. Connecting Automatic Generation Control and Economic Dispatch from an Optimization View. *IEEE Transactions on Control of Network Systems*, Accpected, 2015.

[19] S. H. Low. A duality model of TCP and queue management algorithms. *IEEE/ACM Transactions on Networking*, 11:525–536, August 2003.

[20] S. H. Low and D. E. Lapsley. Optimal flow control, I: Basic algorithm and convergence. *IEEE/ACM Transactions on networking*, 7:861–874, 1999.

[21] Jan M., Janusz W. B., and James R. B. *Power system dynamics: Stability and Control*. John Wiley & Sons, Inc., 2nd edition, 2008.

[22] E. Mallada and S. H. Low. Distributed frequency-preserving optimal load control. *Proceedings of the IFAC World Congress*, 2014.

[23] J. Morren, S. de Haan, W. Kling, and J. Ferreira. Wind turbines emulating inertia and supporting primary frequency control. *IEEE Transactions on Power Systems*, 21:433-434, 2006.

[24] A. J. Wood and B. F. Wollenberg. *Power Generation, Operation, and Control*. John Wiley & Sons, Inc., 2nd edition, 1996.

[25] X. Zhang and A. Papachristodoulou. A real-time control framework for smart power networks with star topology. *Proceedings of American Control Conference*, 2013.

[26] C. Zhao, U. Topcu, N. Li, and S. Low. Design and stability of load-side primary frequency control in power systems. *IEEE Transactions on Automatic Control*, 59:1177–1189, 2014.

[27] C. Zhao, U. Topcu, and S. Low. Swing dynamics as primal-dual algorithm for optimal load control. *Proceedings of IEEE SmartGridComm*, 2012.

[28] L. Chen and S. You. Reverse and forward engineering of frequency control in power networks. *Technical Report*, 2016. Available at http://spot.colorado.edu/∼lich1539/papers/Chen-2016-RFE-TN.pdf.